International Journal of Adhesion & Adhesives 108 (2021) 102872

Contents lists available at ScienceDirect

International Journal of Adhesion and Adhesives

journal homepage: http://www.elsevier.com/locate/ijadhadh

Structure-property relationship of nanostructured functionally graded epoxy adhesives

Olivier Tramis, Bouchra Hassoune-Rhabbour, Valérie Nassiet *

Université de Toulouse, INPT, Laboratoire Génie de Production, Ecole Nationale D'Ingénieurs de Tarbes, 47 Avenue D'Azereix, B.P. 1629, 65016, Tarbes Cedex, France

ARTICLE INFO

Keywords:
Functionally graded adhesive
Epoxy
Adherence
Copolymers
Wedge test
Experimental

ABSTRACT

Adhesives with a variation of properties along the bondline are appealing to the joining industry, yet few developments give easy, versatile implementations and at the same time a control over the toughness of the joints. We herein present an original methodology to control the variation of properties in functionally graded epoxy adhesives (FGAs). The FGAs are obtained by putting into contact two plots of compatible adhesives, where the two plots occupy each half of the aluminum substrates. Diffusion of thermoplastic, triblock copolymers in the epoxy-amine adhesive within the joint provokes a gradient of copolymers, inducing in turn a variation of properties along the overlap. We use a driven wedge test (DWT) to assess the variation of properties within the FGAs, by continuously inserting a wedge in the unbonded part of the sample. We discuss on the contribution of the ductility and resilience of the FGAs to the overall energy dissipated, which is found to be superior for FGAs, compared to homogenously filled adhesives. We infer this result to the heterogeneous spatial distribution of the copolymers in the FGAs, due to the diffusion.

1. Introduction

Ideally, any load applied to an adhesive joint should be evenly distributed along the overlap, meaning an ideal adhesive is not subjected to stress concentrations. Thanks to their graded properties, functionally graded adhesives (FGAs) [1] can smoothen stress distribution and relieve stress concentrations. FGAs thus approach the behavior of an ideal adhesive when used in an adhesive joint. Since the first development of the mixed modulus bond line by Hart-Smith [2], FGAs have been extensively studied numerically [3,4]. Experimentally, various configurations have been proposed. Several authors followed the mixed modulus bond line, by using adhesives with different Young's moduli in the same joints [5,6], or in combination with a variation of bondline thickness or geometry thickness [7]. Modification of the adhesives' properties by addition of fillers have also been proposed. Djilali et al. [8] used rubber microparticles to modify their adhesives' properties. A high strength adhesive was placed at the middle of the joint, while the same adhesive filled with amine terminated polysiloxane (hence more ductile) was placed at the edge. Bonaldo et al. [9] placed an adhesive filled with an arbitrary concentration of thermoplastic, expandable microparticles along the overlap. Higher concentrated adhesives were placed on the edge, the filler's concentration decreasing toward the center. In both studies, FGAs shown higher strength than homogeneously filled adhesives for various single-lap joints (SLJ) configurations. They however noted than the microparticles may act as stress concentrators, possibly degrading the adhesives' properties, limiting the potential of the FGAs. Several authors went a step ahead by selectively placing their microparticles within the bondline [10]. In the one hand, they homogenously fill samples with glass microparticles. In the other hand, they put the microparticles on the edge of the bondline - where the stresses are concentrated in SLJ configuration. They obtain similar strength for uniformly or selectively filled joints, meaning that the stress fields are similar in both configurations. In other instances, the properties of the adhesive were graded by step-wise induction curing, where the time and the temperature of the crosslinking along the bondline's length differed at each step [11]. Induction-cured FGAs were shown to possess higher strength than homogenously cured adhesives in SLJs. Lobel et al. [12] used a thin strap of ductile adhesive within a thermoset adhesive of high strength and stiffness. The ductile adhesive acted as a physical barrier to crack propagation in both SLJs and double cantilever beam configurations, ultimately stopping crack propagation thanks to the toughness mismatch on the crack path. Nakanouchi et al. [13] used a mix of two acrylic adhesives to obtain a graded joint, where the graduation could be varied by varying the mixing ratio.

* Corresponding author.
E-mail address: valerie.nassiet@enit.fr (V. Nassiet).

https://doi.org/10.1016/j.ijadhadh.2021.102872

Available online 3 April 2021

Our contribution is focused on the design of an original methodology to control the properties' variation in functionally graded epoxy adhesives (FGAs). FGAs are designed by the use of nanostructured epoxy-amine adhesives. Nanostructuration is obtained by mixing thermoplastic triblock copolymers to an epoxy-amine adhesive. We use one adhesive as the basis, and two different kind of copolymers. For similar epoxy-amine systems, Chen et al. [14] and Brethous et al. [15] showed that the copolymers ensure an increase of toughness with an upkeep of both the glass transition temperature and the Young's modulus. FGA joints are obtained as follows: the copolymer filled adhesive is put in contact with the neat adhesive within the same joint. Upon contact, thermodynamically driven diffusion of the copolymers occurs, without external intervention other than the temperature during the curing cycle. We assess the graduation of properties by continuously inserting a wedge into the unbonded part of the samples, namely a driven wedge test (DWT) [16]. The DWT is a mechanical test able to create several crack jumps over a short overlap length, compared to the classical DCB. The DWT was chosen over SLJ as the latter only gives an average joint strength. Thanks to the DWT, each crack jump can be analyzed in terms of the local properties of the adhesive, at the position of the crack in the joints. We make experimental quantitative comparisons between both non-filled and homogeneously filled adhesive joints, and FGAs. We finally attempt to relate the spatial distribution of the copolymers to the measured increase of resilience in FGAs through the DWT.

2. Experimental

Samples are made from two anodized aluminum substrates, bonded with epoxy-amine adhesives, either neat, filled or graded (Fig. 1).

2.1. Materials

Epoxy-based solid resins DER332 (DiGlycidylEther of Bisphenol-A, DGEBA), supplied by Sigma-Aldrich (Sigma-Aldrich, France), was mixed with a tri-amine hardener, namely MDEA (4,4′-Methylenebis(2,6-DiEthylAniline), provided by Lonzacure, (France). M52 and M22N "Nanostrength®" copolymers were provided by Arkema (France). The M52 is a triblock copolymer (PMMA-*b*-PBA-*b*-PMMA) (Poly(Methacrylate de Methyl)-*b*-Poly(Butyl Acrylate)-*b*-Poly(Methyl Methacrylate)). The M22N is a triblock copolymer as well, with DMA(DiMethylAcrylamide) grafted onto the PMMA blocks (PMMA-co-DMA-b-PBA-b-PMMA-co-DMA), in order to increase its miscibility with the DGEBA [17].

The key feature of the copolymers comes from the thermodynamic compatibility of the PMMA blocks with the DGEBA, while the PBA is not. During copolymers incorporation, a nanoscale phase separation occurs, which leads to an increase of toughness (K_{IC}) with an upkeep of glass transition temperature (T_g) [15] (Table 1).

The reference adhesive was obtained by vigorously mixing the DGEBA resin with the MDEA hardener in stoichiometric ratio (1:0.31), until the mixture was homogeneous.

Nanostructured adhesives were obtained by incorporating 10%wt of either the M52 or M22N copolymers within the DGEBA. Small amounts of copolymers were introduced sequentially into the DGEBA. Then, MDEA was added. The nanostructured adhesives were codenamed after their copolymer content: the adhesive containing M52 copolymers was referred to as M52. Similarly, the adhesive containing M22N copolymers was referred to as M22N.

Aluminum substrates (2017 alloy, sometimes referred to as AU4G, Asmobax, France) were received at their final dimensions, as illustrated on Fig. 1, (a). The substrates were chosen thinner from usual wedge tests (as described in ASTM D 3762 and ISO 10354), since the environment had no time to influence the outcomes of the driven wedge tests. One end of the substrate was machined at 30°, to make wedge insertion easier. They were treated by phosphoric anodization (PAA), by immersing them in a phosphoric acid solution (10% by weight of H_3PO_4), under low current and voltage (0.5 A, 20 V) during 20 min, then rinsed in distilled water at room temperature. The anodized substrates were placed in a desiccator for 1 h, to allow the surface to completely dry. Prior to bonding, PTFE (PolyTetraFluoroEthylene) inserts of thickness of 0.1 mm ± 0.015 mm were deposited on the extremities of each substrate (Fig. 1, (a)). They were then bonded with the adhesives, as illustrated on Fig. 1(c) and (d). In the case of a FGA, the nanostructured adhesive was spread on the one side of the substrate, far from the machined end (Fig. 1, (d)), for an initial bondline of 20 mm. The reference adhesive was then spread on the other half of the substrate, for

Table 1
Relevant data of the bulk adhesives, from Brethous et al. [15].

Adhesives	Reference	M52	M22N
Gelation time at 160 °C (min)	36 ± 1	19 ± 1	40 ± 3
Young's modulus (GPa)	2.73 ± 0.03	2.55 ± 0.03	2.61 ± 0.03
T_g (°C)	167 ± 3	170 ± 3	164 ± 3
K_{IC} (MPa.m$^{1/2}$)	0.89 ± 0.04	1.24 ± 0.12	0.98 ± 0.05

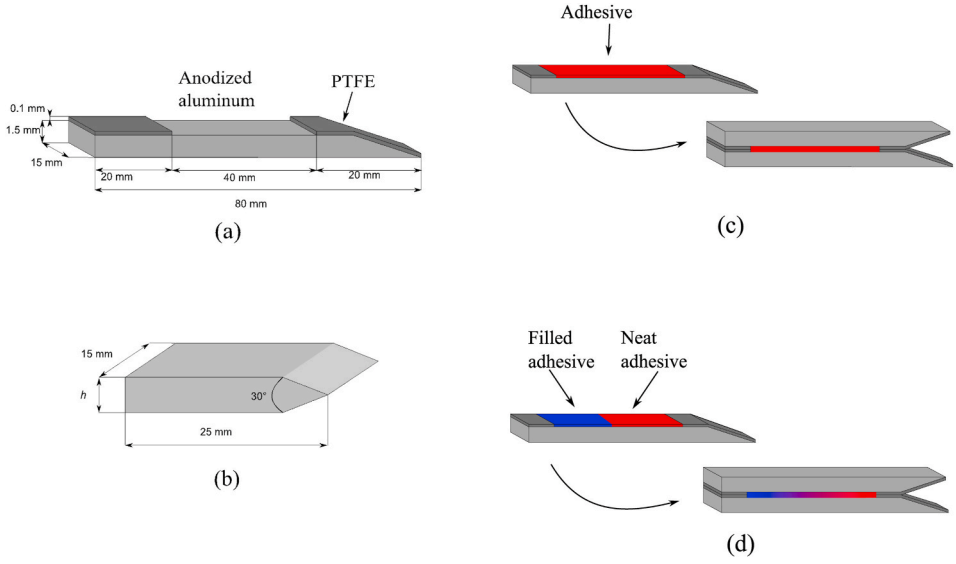

Fig. 1. (a) Dimensions of the aluminum substrates. (b) Dimensions of the wedges. See text for the thickness, *h*. (c) Protocol to bond mono-adhesive joints. (d) Protocol to bond FGAs joints.

an initial bondline of 20 mm. The graded properties arose from diffusion of the copolymers contained in the filled adhesive toward the neat adhesive, which begun as soon as contact was made between the neat and the filled adhesives. Thus, during a driven wedge test, a crack would initiate in the neat side of the joint, and propagate toward the filled adhesive. FGA made of the reference and M52 adhesives are referred to as "FGA 1" in the following. "FGA 2" holds for FGA made of the reference and M22N adhesives.

The adhesively bonded samples were clamped on a custom setup, and put in a pre-heated oven at 160 °C, for 4 h, followed by a 75 min post-curing stage at 190 °C. Cooling down was performed at a 2 °C/min rate to room temperature.

Wedges were machined at the laboratory (25 × 15 mm^2), from a thin steel sheet. Adams et al. [18] stated that friction is the main issue of a driven wedge test. To minimize friction, the wedges were covered with the same PTFE film as used for the samples. Thus, friction was only made between PTFE surfaces during the driven wedge test experiments.

2.2. Methods

Mechanical tests were performed on a universal tensile test machine (Instron). The samples were fixed on the lower crosshead, and the wedge was fixed on the upper traverse (Fig. 2, (a)), linked to a 500 N load cell. The force applied by the machine to the wedge was recorded alongside the wedge's displacement. Optical cameras, with a resolution of 1600 × 1230 pixels, were used to record image sequences of both crack creation (1 image/second) and propagation steps (6 images/second), on both sides of the sample. Digital Image Correlation (Fig. 2, (b)) (DIC, Aramis 2 M, Gom®) was used to determine crack length with a resolution of 50 μm. The crack tip was determined as the point of zero displacement [19, 20]. The tip of the crack is taken when the zone ahead of the crack vanishes from red (tension) to blue (neutral) on Fig. 2, (d), determined numerically.

2.2.1. Crack creation test setup

Crack creation was performed with a 0.7 mm thick PTFE-wrapped wedge. The wedge was driven at a constant velocity of 0.1 mm/s. This set of parameter allowed a crack to be created in the reference adhesive in a reproducible manner. Qualitative comparison of the bonded samples was made by measuring the length of adhesive cracked by DIC.

The amount of strain, ε, underwent by the outer surface of the substrate at the crack tip may be estimated as follows [21].

$$\varepsilon = \frac{3\Delta h}{2a^2} \quad (1)$$

With Δ the wedge's half-thickness (symmetric wedge test), h the substrate's thickness and "a" the crack length.

In the case of the M22N adhesive (the adhesive requiring the highest load to crack), taking "a" at the onset of crack propagation (see L_i in sections 3.2 and 3.3 for its respective values used in the computation), it follows after equation (1) that $\varepsilon = 0.006$ and $\varepsilon = 0.0135$ of strain during the initiation and forced propagation, respectively. By definition, the "plastic yield point" is the point at which a materials begins to undergo plastic deformation, and is usually taken at 0.02 of strain for aluminum alloys, meaning that the substrate did not yield at any points during our experiments.

2.2.2. Driven wedge test setup

The reference adhesive being the more brittle, it was used in preliminary experiments to determine parameters that gave an error less than 10% on the final crack length, L (see Table 2).

The forced crack propagation step was ensured by a PTFE-covered wedge of 1.2 mm final thickness. A thicker wedge was used for the forced crack propagation in order to compensate that the adhesively bonded sample was pre-cracked, knowing that the forced propagation was stopped before the wedge reached the adhesives. The wedge was inserted at a constant velocity of 1 mm/s, and stopped just before the wedge went into contact with the bonded part of the samples. Thus, according to Fig. 1, (a), the wedge was driven on about 20 mm. We verified by Digital Image Correlation that between each crack jump, the

Table 2
Length of cracked adhesive at the end of a DWT. Data is representative of six samples per adhesive.

Adhesives	Reference	M52	FGA 1	M22N	FGA 2
Total length of cracked adhesive (mm)	25.9 ± 0.5	21.8 ± 0.3	21.9 ± 1	26.2 ± 3.2	25.4 ± 3.4

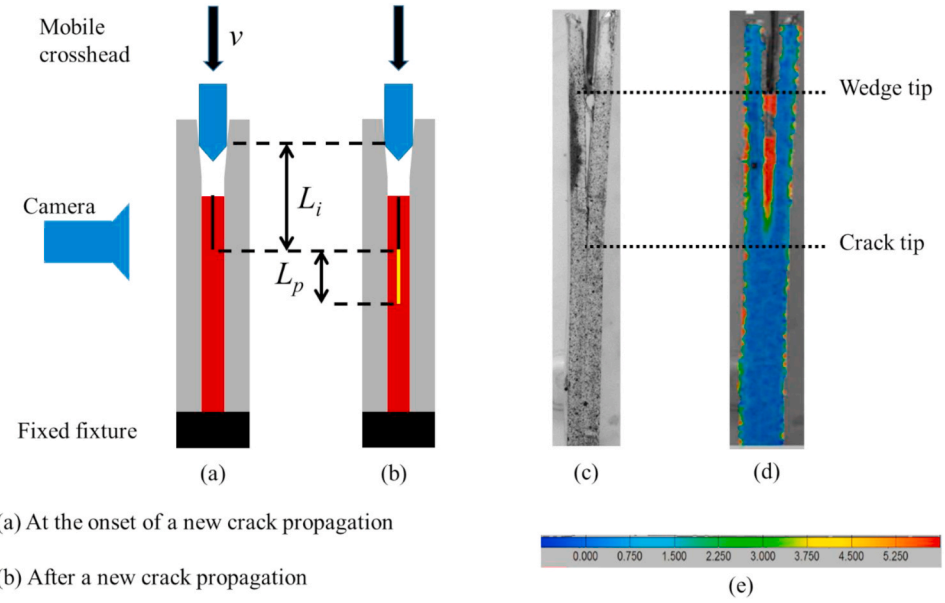

Fig. 2. (a, b) Sketch of the setup used for the study. See section 2.2.2 for the definition of L_i and L_p. (c) Original image. (d) Post-treated image showing the deformation field of a running test by Digital Image Correlation, with (e) its associated color bar, representing the numerically estimated major strain. (For interpretation of the references to color in this figure legend, the reader is referred to the Web version of this article.)

crack was not moving. It is an important feature, meaning that when the wedge progresses, the crack front remains still, and thus the potential energy at the onset of crack propagation is only due to the substrates bending and stored potential energy in the adhesive. Similarly, we checked by DIC that crack propagation was much faster than the wedge's insertion velocity. It is another key feature, meaning that crack propagation is only due to the release of the energy stored prior to the crack propagation.

In this work, we choose not to work on the full, final crack length, L, nor on the toughness (i.e., the impact resistance) nor the fracture energy. We instead propose to divide the crack length into two lengths ($L = L_i + L_p$), representing the ductility and resilience contribution of the adhesive to the joint fracture.

We define the ductility as the ability of an adhesive to accumulate elastic –potential – energy prior to crack progression. As depicted on Fig. 2 (a) and Fig. 2, (d), L_i, the initiation length, is defined as the distance between the wedge tip and the crack tip, *taken at the onset of crack propagation*. A short L_i means strongly bent substrates, revealing an adhesive of high ductility.

We define the resilience as the ability of an adhesive to dissipate the accumulated energy through the creation of a new surface. As depicted on Fig. 2, (b), L_p, the length on which the adhesive cracked after crack propagation, is a witness of an adhesive's resilience. A joint cracked on a short L_p is a highly resilient adhesive, meaning it can dissipate a large amount of accumulated energy by creating a small amount of new surface.

2.2.3. Infrared spectroscopy

The infrared spectra were obtained using a Fourier Transform Infra-Red spectrometer in Attenuated Total Reflection mode (ATR-FTIR) (Spectrum One, PerkinElmer, France). Each spectrum was scanned 4 times from 650 to 4000 cm^{-1}, with a resolution of 4 cm^{-1} and 10 μm penetrating depth (manufacturer specifications). Normalization was done on the absorption band at 1508 cm^{-1} (C═C ring stretch vibration in epoxy prepolymers). The copolymers (both M52 and M22N) exhibited an absorption band at 1730 cm^{-1}, attributed to the C═O vibration of the PMMA blocks. Diffusion validation was made *post-mortem* on cured and cleaved assemblies, by assessing the intensity of this particular band at different points of the overlap length.

Relative comparisons of band intensity were computed as follows:

$$\text{Intensity at given point} = \frac{\left(\frac{Abs(1730)}{Abs(1508)}\right)\text{point}}{\left(\frac{Abs(1730)}{Abs(1508)}\right)\text{ref}} \quad (2)$$

The 1730 cm^{-1} band was chosen for comparison. The reference ratio was taken in the initially filled part of the FGA, far from the initial border (position "1" as defined in Fig. 3). Equation (2) thus gave a relative intensity, which was used to assess copolymers diffusion in FGAs.

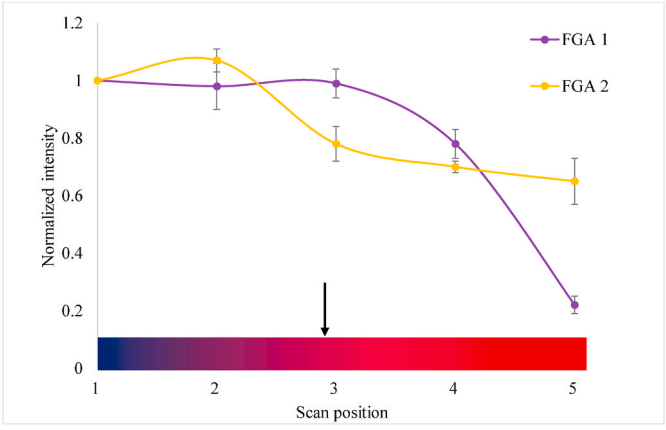

Fig. 3. FTIR analysis of FGA 1 and FGA 2. Six samples per adhesive were scanned. The black arrow indicates the position of the initial border. Diffusion occurred from point 1 to point 5. Lines are guide for eyes.

3. Results

3.1. Post-mortem FTIR validation of diffusion

The first part of the study focused on the diffusion phenomenon. ATR-FTIR was used to follow the copolymers diffusion *post-mortem* (i.e., on already cured and cleaved samples) on the whole overlap length.

The band intensity is represented for each FGA in Fig. 3. Intensities were computed using equation (2).

The points labeled "1" and "2" were scanned in the filled part, respectively far from and close (*ca.* 1 mm) to the initial border. The point labeled "5" was taken at *ca.* 1 mm far of the PTFE insert, in the neat part, far from the initial border. Points labeled "3" and "4" were scanned within the initial neat part, moving away from the initial border.

For both FGAs, the intensity gradually decreased as the scans proceeded from the filled part to the neat part. The intensity at point "5" was non-nil, which meant copolymers were indeed present in the reference part of the joint, confirming that diffusion occurred.

The trends observed on Fig. 3 might be seen as a competition between crosslinking and diffusion. Indeed, from Table 1, it can be seen that the gelation time is shorter for the M52 adhesive.

In the FGA 1 samples, the copolymer distribution was highly non-linear along the overlap. The part of the sample labeled "1" on Fig. 3 reached its gel state first, followed by point 2, then point 3, and so on, gradually reducing the space left for diffusion, since it only occurred before gelation. Crosslinking was faster than diffusion overall, the gelation trapping the copolymers before they can diffuse far in the neat part. Therefore, the copolymers detected from point "3" diffused before the M52 part reached its gel state. Only copolymers that were able to reach point 3 before the gelation were able to reach point 4 and 5, hence the rapid decrease measured after point 3.

In the FGA 2 samples, the decrease in copolymers was more regular along the overlap. M22N copolymers had more time to diffuse since the gelation time of the M22N adhesive is of the same magnitude as the reference one.

The final position reached by the cracks at the end of a DWT within the bonded part are reported in Table 2, for each adhesive. It shall be reminded that the wedge was pushed on a distance of 20 mm, which corresponds to the unbonded, PTFE-wrapped part of the substrate. Table 2 shows that cracks for all samples stopped after the initial border (slightly after point "3" depicted on Fig. 3).

3.2. Crack creation step

Crack initiation lengths, measured right after crack creation, are reported on Fig. 4. Six samples per adhesive were tested. The cracks systematically stopped between point "4" and point "5" (Fig. 3), independently of the nature of the adhesive. All the failures were cohesive in the bulk of the adhesive, for all adhesives.

The reference adhesive had the highest uncertainties, explained by its high brittleness. The M52 and M22N adhesives had lower uncertainties. On Fig. 4, (a), their initiation lengths were shorter than the reference's, and the loads needed to reach the onset of crack propagation were higher. Thus, the M52 and M22N adhesive were more ductile than the reference. On Fig. 4, (b), the initiated crack propagated on higher distances (on average) than the reference. This may be explained by the fact that they stored a higher amount of bending energy. Despite a higher resilience, they had a surplus of energy to dissipate, hence a longer cracked adhesive length.

Based on Fig. 4 (a) and Fig. 4, (b), FGAs were almost as ductile as the reference and almost as resilient as the M52 or M22N adhesive. FGAs therefore presents an interesting balance between ductility and resilience, as if a lower ductility is compensated by a higher resilience.

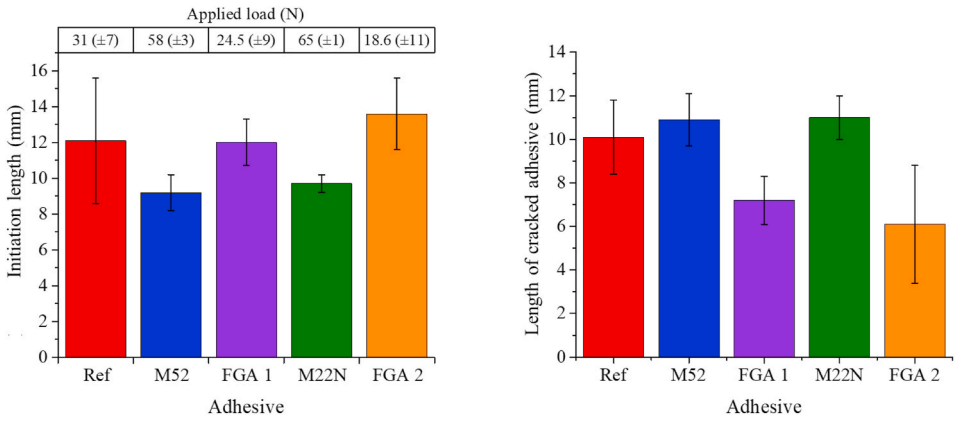

Fig. 4. (a) Initiation length prior to crack creation, L_i. Upper table represents the applied load to initiate a crack. (b) Length of cracked adhesive, L_p. Six samples per adhesive were tested.

The crack creation study showed two important features. Firstly, dividing the crack length into an initiation and a propagation contribution provides a crack propagation interpretation oriented from the adhesives' point of view. While ductility and resilience are certainly intertwined in a more complex way, splitting the crack length gives additional, relevant information on both ductility and resilience contributions to the crack propagation, thus putting the adhesives in the core of the analysis. Indeed, if we had computed the usual crack length, L ($L = L_i + L_p$), both FGAs have $L = 20$ mm, M52 and M22N adhesives have $L = 21$ mm and the reference adhesive has L = 22 mm for the crack creation. Given that uncertainties are about 2 mm, the measure of L alone is blind to the ductility and resilience contributions, and we would have skipped important, fundamental features seen by splitting L as $L_i + L_p$. Secondly, FGAs point to an interesting balance of ductility and resilience. This balance seems to be a key feature of our FGAs, even if this only step does not entirely describe it. This justifies the need to use a test able to reveal the graded properties of the FGAs, topic of the next section.

3.3. Forced crack propagation study

Once pre-cracked, the samples were subjected to forced propagation. During a driven wedge test, loading and releasing events (i.e., crack jumps) may appear, as seen on Fig. 5 and Fig. 6. We tested six samples per adhesive, but only trends are shown for the sake of clarity.

The curves of Figs. 5 and 6 offer many insights about the adhesives' properties.

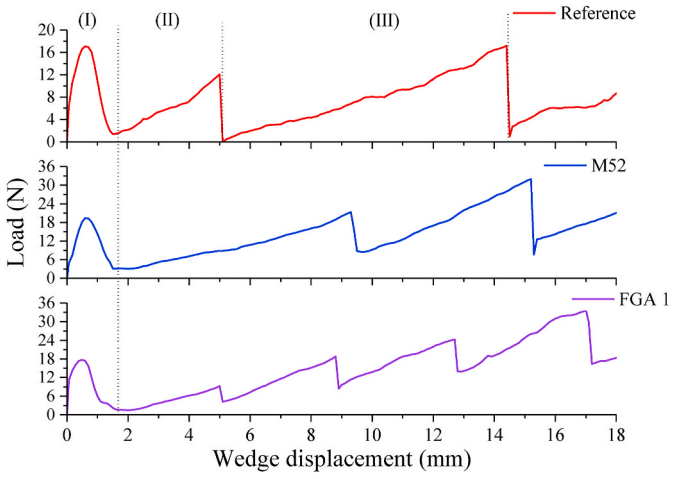

Fig. 5. Trends of load versus wedge displacement, for the reference/M52 system.

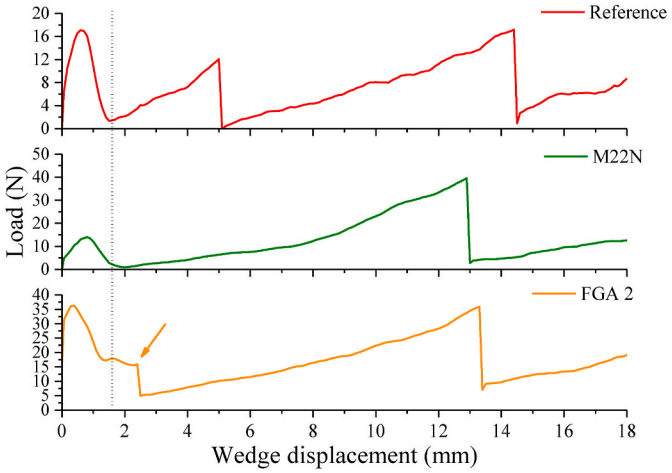

Fig. 6. Trends of load versus wedge displacement, for the reference/M22N system. The arrow indicates a crack jump.

First, the wedge was inserted between the substrates. This is seen in step (I) (Fig. 5), where the load built up. The load then dropped and the substrates begun to bend. The force gradually built up, then suddenly dropped (step (II)) (Fig. 5). The clear drop in load shows a crack propagation event (indicated by an arrow for the FGA 2 joint on Fig. 6). The force did not drop to zero, due to the arms of the substrate compressing the wedge during the test, thus giving an offset to the starting force. The wedge was still advancing, seen by the force that built up again, until sufficient elastic energy had been stored within the arms (step (III)) (Fig. 5). A new crack propagation occurred, as seen by a new drop of force. The force associated with the last event always seemed to be higher than the first event. It shall be noted that the force recorded at the events during the test was systematically higher for both M52 and M22N adhesives, as for the crack initiation step. The force associated to the FGA adhesives (FGA 1 and FGA 2) varied between the force of the reference adhesive and the associated nanostructured adhesives.

The distance between two events may allow for discriminating the resilience of the adhesives: the shorter the distance, the more resilient the adhesive. From Fig. 5, the distance between two events was much shorter for the FGA 1 joints than the M52 joints, which is the toughest adhesive used herein (see Table 1). From Fig. 6, however, the distance between two events for FGA 2 joints was longer than the reference joint.

Additionally, a late event may be the witness of a high ductility. Both FGA 1 and FGA 2 joints had their first event as early as the reference adhesive, and earlier than the associated M52/M22N adhesives. The

M22N had a noteworthy feature, as only one crack jump was systematically recorded. Because of its ductility, it appears that its resilience seems less than other the adhesives. The reason behind this behavior may be explained as follows.

Chen et al. [14] showed, for an anhydride-cured DGEBA, that both the ratio of immiscible to miscible (ITM) copolymers block, as well as the degree of miscibility of the miscible block have direct influence on the copolymers' morphology, which was related to the toughness.

For a given ITM ratio, an increase in miscibility of the miscible block yields a well-dispersed worm-like micelle arrangement. This was shown to be the case with M22N copolymers, which have DMA grafted to their PMMA block to increase the M22N copolymers' miscibility.

At similar miscibility, a higher ITM ratio translates to a finer arrangement of vesicles, at a sub-micrometer scale. This was shown to be the case with M52 copolymers, which have a longer PBA (immiscible) block, thus a higher ITM ratio than the M22N copolymers.

Dean et al. [22] reported that copolymers forming vesicles exhibit a higher increase of toughness than micellar arrangement of copolymers.

Therefore, for our adhesives, we suppose that a higher copolymer miscibility gives an adhesive with a higher ductility (e.g. M22N). A higher ITM ratio shall give a more resilient adhesive (e.g. M52) following this simple reasoning. As a consequence, the recorded accumulation of potential energy prior to crack by the M22N provoked a crack much longer than anticipated from the toughness value (cf. Table 1), hence a single crack jump systematically recorded. For its second crack jump, the FGA 2 joints share the same feature.

To gain further insight about the characterization of the FGAs' graded properties by the DWT, division of the crack length into two contributions was applied as well for all events, which are made of an initiation step, represented by the substrates' bending length at the onset of crack propagation (L_i). Contrarily to the L_p depicted on Fig. 2, we measure here the adhesive cracked length as the distance between the crack tip at the onset of crack propagation, and the position of the crack after crack propagation, i.e. *crack jumps*.

Crack initiation lengths (L_i) are reported on Fig. 7, while crack jumps are reported in Table 3.

By comparing reference and nanostructured adhesives, for each event, the associated L_i is systematically shorter for the nanostructured adhesives, indicating a greater ductility. The crack jumps are longer for the M22N adhesives, for the same reasons as discussed earlier. Another noteworthy feature is that both L_i and L_p are constant for a given mono-adhesive, indicating that both reference and nanostructured joints are homogeneous, i.e. of constant ductility and resilience along the overlap.

It appears clearly from Fig. 7 that the FGAs possess varying properties along their overlap. The crack initiation lengths for the FGAs are not equal for each event. This may be straightforwardly explained by the fact that the copolymers' concentration increases at each event. Thus, the ductility of the FGAs increases at each crack onset, reflected by shorter L_i measured. From Table 3 however the crack jumps are constant for both FGAs. We would have expected to measure a decreasing L_p value, since the copolymers' concentration is supposed to increase. This feature will be discussed in the next section.

In this section we showed that the driven wedge test (DWT) is a relevant tool to evaluate the homogeneity of an adhesive joint. Through the DWT, we demonstrated that our FGAs possess a gradient of property along their overlap. In the next section we attempt to clarify how the gradient of copolymers impacts the ductility and resilience of our FGAs.

4. Discussion

The elastic potential energy, U_E, stored in the bent arms and associated to the initiation length L_i, is given in equation (3). With E the substrates' Young modulus, "b" and "e" the substrates' respective width and thickness, and "h" the wedge's thickness, equation (3) is derived from the simple beam theory [23], and is used only for comparison purpose

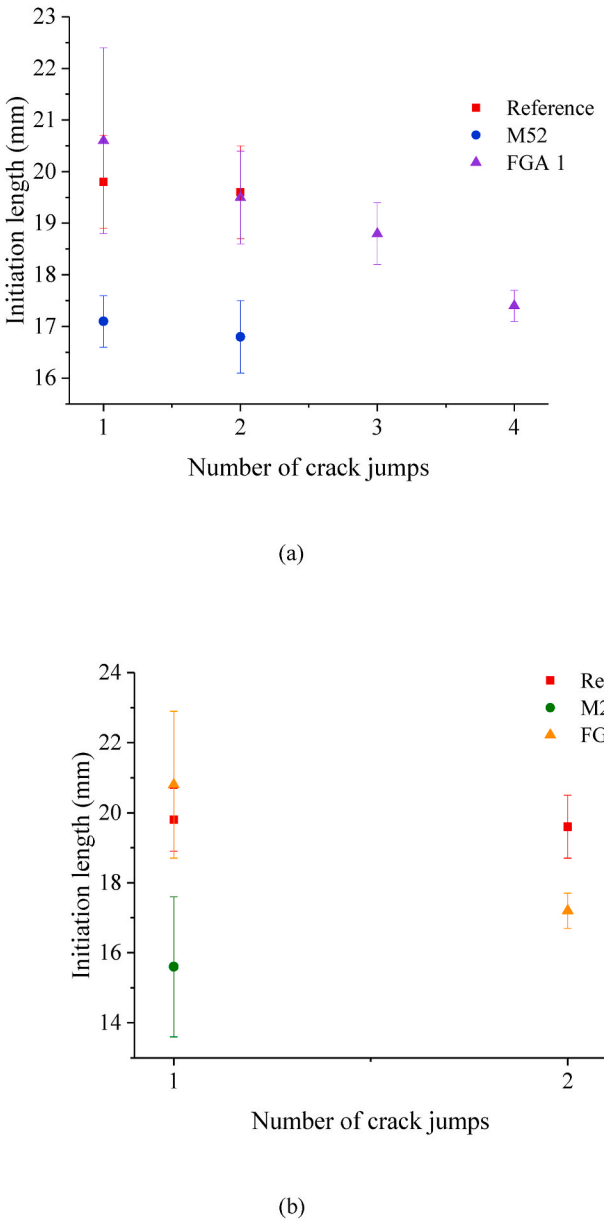

Fig. 7. Initiation length associated with each adhesive tested. (a) Reference/M52 system. (b) Reference/M22N system.

Table 3
Adhesive cracked length, L_p, all samples tested.

Adhesives	Reference adhesive	M52	FGA 1	M22N	FGA 2
Mean crack jump (mm)	5 ± 0.1	4.5 ± 0.5	3.5 ± 0.5	11 ± 1	8.8 ± 3

$$U_E = \frac{Ebe^3h^2}{4L_i^3} \tag{3}$$

This energy is computed by supposing that the substrates behave as built-in beams, to simplify computation. The true value of the energy requires more complex computations, to take into account either slip and shear at crack tip (root rotation), or the adhesive compliance (elastic foundation).

The reference and the nanostructured adhesive joints exhibit the interesting feature of all crack jumps being equals (Table 3). This feature

is explained by the fact that they are homogeneous joints, feature highlighted using the same method by Dillard et al. [16]. It is therefore normal that the potential energy is consistent between crack jumps, since both ductility and resilience are constant along the overlap.

It is clear from Fig. 8 that the potential energy required to initiate an event in FGAs increases for each event. From Table 3, FGAs display two interesting features. Firstly, the crack jumps are smaller than for the nanostructured adhesives. More surprisingly, the mean surface created after each crack jump for the FGAs is constant. Indeed, a higher copolymers' concentration would imply a greater resilience, then a shorter L_p. Since the amount of stored energy increases at each crack jump, it results in a longer L_p than anticipated. Thus the consistency of L_p is the striking result of a balance between ductility and resilience.

The nanostructured adhesives may be seen as a reference adhesive, homogeneously filled with copolymers, while FGAs may be seen as reference adhesives with a heterogeneous spatial arrangement of copolymers, due to their diffusion (Fig. 3). In the case of epoxy matrices reinforced by thermoplastic block copolymers, Kinloch et al. Pearson et al. and Chen et al. [14,24,25], amongst others, showed that a higher toughness resulted from cavitation of the copolymers, followed by a subsequent plasticization of the matrix. Those phenomena may explain the increased toughness of the nanostructured adhesives. In the case of the FGAs, at each crack jump, a crack encounters more copolymers, changing the energy balance. Thus, cavitation of copolymers and subsequent plasticization occur more often, increasing the overall energy to initiate and propagate a crack within.

Further explanations in the sense that copolymers organization is the main reinforcing feature may be drawn. Dean et al. [22] showed that the fracture energy (i.e., G_c) may be related to the interparticles distance between copolymers. They showed that the fracture energy depends not on the weight concentration of block copolymers but on the size and morphology of the copolymers. Particularly, the ratio of the interparticles distance to the diameter of the vesicles (either spherical or micellar) was shown to be inversely proportional to the fracture toughness, i.e. smaller interparticles distance led to a greater fracture energy enhancement. They suggested that a smaller ratio (i.e., a smaller interparticles distance for a specific particle morphology) gave a greater enhancement on the fracture energy. Possible mechanisms were thought to be a change of stress state upon cavitation of the particles, from plane strain to plane stress, since for a short interparticles distance, the in-between epoxy would be easier to plastically deform. They also hypothesized that the stress field around the particles would overlap if the particles are close enough, which would facilitate and enhance matrix plasticization.

In the case of our FGAs, the diffusion of copolymers may induce a gradient of interparticles distance, since fewer copolymers could diffuse to the neat part (point "5" of Fig. 3) than to the border (point "2" of Fig. 3). Fewer particles in the neat part means longer interparticles distance, since this value should be controlled by the diffusion. Thus, the more the crack penetrated within the FGAs, the smaller the interparticles distance became. At each crack jump, the crack tip met more copolymers with a denser packing, increasing the effective stress field and surrounding stress field overlap ahead. Thus, the DWT in a FGA is equivalent to as many crack initiation of a new, more resilient adhesive as crack jumps recorded.

As a brief summary, we showed that our FGAs approach the behavior of optimal adhesives, through a fine balance of ductility and resilience. Compared to homogeneous joints, they accumulate less energy at each event, but dissipate it earlier, which allow them to accumulate energy again at a faster pace. Thus, for given parameters, more events mean more energy dissipated.

5. Conclusion

We proposed a new kind of functionally graded adhesives, where the properties' gradient was the result of the design of thermodynamically driven copolymers diffusion (i.e., passive diffusion). Diffusion was validated by infrared spectroscopy, which showed the presence of copolymers along the overlap. The diffusion was found to be dependent of the gelation kinetic. As a consequence, the graduation also resulted from this kinetic.

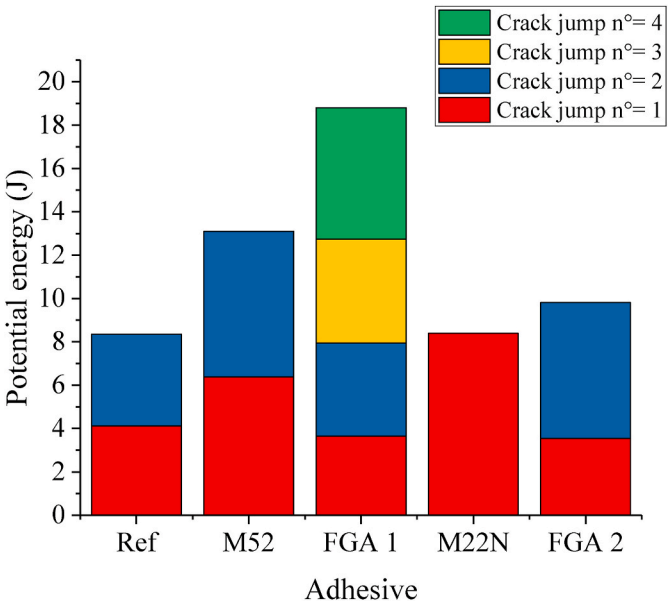

Fig. 8. Potential energy required to initiate each crack jumps during a driven wedge test, as well as its total amount. Uncertainty on the values displayed is *ca.* ± 0.75 J.

The performance of the graded joints in terms of forced-crack propagation resistance was compared to homogeneous adhesive joints by the driven wedge test. Firstly, dividing the crack length into an initiation length (L_i) and a propagation length (L_p) ensures relevant information on both ductility and resilience contributions to the crack propagation not highlighted with the only analysis of the usual crack length, L, which is quasi-equal whatever the adhesive. It was shown that the graded joints possess a superior "effective" resilience, with FGA 1 joints showing the highest resilience. Since the kinetics of the copolymer diffusion was faster for FGA 1 joints than for FGA 2 joints, FGA 1 had a greater copolymers' concentration gradient. At each crack jump, a crack encountered more copolymers in FGA 1 joints than in FGA 2 joints, modifying more the energy balance. Hence, the overall energy to initiate and propagate a crack within was greater for FGA 1 joints than FGA 2 joints. Then, the local increase of resilience is attributed to heterogeneous spatial and conformational arrangements of the copolymers along the overlap.

Declaration of competing interest

None.

Data statement

Datasets will be made available upon reasonable requests.

References

[1] Marques JB, Barbosa AQ, da Silva CI, Carbas RJC, da Silva LFM. An overview of manufacturing functionally graded adhesives–Challenges and prospects. J Adhes 2019:1–35. https://doi.org/10.1080/00218464.2019.1646647.
[2] Hart-Smith LJ. Adhesive-bonded double-lap joints. 1973. NAS1-11234.
[3] Cassano AG, Stapleton SE, Schmidt DF. Functionally graded adhesives joints with enhanced strength. AIAA Scitech 2019 Forum 2019:234. https://doi.org/10.2514/6.2019-0234.

[4] Stapleton SE, Cassano AG, Najafian S, Schmidt DF. Functionally graded adhesives using radiation curing. AIAA Scitech 2020 Forum 2020:1929. https://doi.org/10.2514/6.2020-1929.
[5] Pires I, Quintino L, Durodola JF, Beevers A. Performance of bi-adhesive bonded aluminium lap joints. Int J Adhesion Adhes 2003;23:215–23. https://doi.org/10.1016/S0143-7496(03)00024-1.
[6] Fitton MD, Broughton JG. Variable modulus adhesives: an approach to optimised joint performance. Int J Adhesion Adhes 2005;25:329–36.
[7] da Silva LFM, Adams RD. Adhesive joints at high and low temperatures using similar and dissimilar adherends and dual adhesives. Int J Adhesion Adhes 2007;27:216–26. https://doi.org/10.1016/j.ijadhadh.2006.04.002.
[8] Djilali T, Nassiet V, Hassoune-Rhabbour B. Graft interpenetrating continuous epoxy-polysiloxane polymeric network. Key Eng Mater 2010;446:111–9. https://doi.org/10.4028/www.scientific.net/KEM.446.111.
[9] Bonaldo J, Banea MD, Carbas RJC, Da Silva LFM, De Barros S. Functionally graded adhesive joints by using thermally expandable particles. J Adhes 2019;95:995–1014. https://doi.org/10.1080/00218464.2018.1456338.
[10] Stapleton SE, Waas AM, Arnold SM. Functionally graded adhesives for composite joints. Int J Adhesion Adhes 2012;35:36–49. https://doi.org/10.1016/j.ijadhadh.2011.11.010.
[11] Carbas RJC, Da Silva LFM, Critchlow GW. Adhesively bonded functionally graded joints by induction heating. Int J Adhesion Adhes 2014;48:110–8. https://doi.org/10.1016/j.ijadhadh.2013.09.045.
[12] Löbel T, Holzhüter D, Sinapius M, Hühne C. A hybrid bondline concept for bonded composite joints. Int J Adhesion Adhes 2016;68:229–38. https://doi.org/10.1016/j.ijadhadh.2016.03.025.
[13] Nakanouchi M, Sato C, Sekiguchi Y, Haraga K, Uno H. Development of application method for fabricating functionally graded adhesive joints by two-component acrylic adhesives with different elastic moduli. J Adhes 2019;95:529–42. https://doi.org/10.1080/00218464.2019.1583562.
[14] Chen J, Taylor A. Epoxy modified with triblock copolymers: morphology, mechanical properties and fracture mechanisms. J Mater Sci 2012;47:4546–60. https://doi.org/10.1007/s10853-012-6313-6.
[15] Bréthous R, Nassiet V, Hassoune-Rhabbour B. Models of adhesive bonding of hybrid structures. Key Eng Mater 2013;550:143–55.
[16] Dillard DA, Pohlit DJ, Jacob GC, Starbuck JM, Kapania RK. On the use of a driven wedge test to acquire dynamic fracture energies of bonded beam specimens. J Adhes 2011;87:395–423. https://doi.org/10.1080/00218464.2011.562125.
[17] Maiez-Tribut S, Pascault JP, Soule ER, Borrajo J, Williams RJJ. Nanostructured epoxies based on the self-assembly of block Copolymers : a new miscible block that can Be tailored to different epoxy formulations. Macromelecules 2007;40:1268–73. https://doi.org/10.1021/ma062185l.
[18] Adams RD, Cowap JW, Farquharson G, Margary GM, Vaughn D. The relative merits of the Boeing wedge test and the double cantilever beam test for assessing the durability of adhesively bonded joints, with particular reference to the use of fracture mechanics. Int J Adhesion Adhes 2009;29:609–20. https://doi.org/10.1016/j.ijadhadh.2009.02.010.
[19] Sargent JP. Durability studies for aerospace applications using peel and wedge tests. Int J Adhesion Adhes 2005;25:247–56. https://doi.org/10.1016/j.ijadhadh.2004.07.005.
[20] Creton C, Ciccotti M. F racture and adhesion of soft materials : a review. Rep Prog Phys 2016;79:046601. https://doi.org/10.1088/0034-4885/79/4/046601.
[21] Budzik M, Jumel J, Imielienska K, Shanahan MER. Accurate and continuous adhesive fracture energy determination using an instrumented wedge test. Int J Adhesion Adhes 2009;29:694–701. https://doi.org/10.1016/j.ijadhadh.2008.11.003.
[22] Dean JM, Grubbs RB, Saad W, Cook RF, Bates FS. Mechanical properties of block copolymer vesicle and micelle modified epoxies. J Polym Sci, Part B: Polym Phys 2003;41:2444–56. https://doi.org/10.1002/polb.10595.
[23] Cognard J. The mechanics of the wedge test. J Adhes 1986;20:1–13. https://doi.org/10.1080/00218468608073236.
[24] Kinloch AJ, Shaw SJ, Hunston DL. Deformation and fracture behaviour of a rubber-toughened epoxy: 2. Failure criteria. Polymer (Guildf) 1983;24:1355–63. https://doi.org/10.1016/0032-3861(83)90071-X.
[25] Pearson RA, Yee AF. Influence of particle size and particle size distribution on toughening mechanisms in rubber-modified epoxies. J Mater Sci 1991;26:3828–44. https://doi.org/10.1007/BF01184979.